Journal of Sound and Vibration 329 (2010) 3470–3483

Contents lists available at ScienceDirect

Journal of Sound and Vibration

journal homepage: www.elsevier.com/locate/jsvi

Sound radiation from real airfoils in turbulence

William J. Devenport [a,*], Joshua K. Staubs [a], Stewart A.L. Glegg [b]

[a] Virginia Tech, Aerospace and Ocean Engineering Department, 215 Randolph Hall, Blacksburg, VA 24061, USA
[b] Florida Atlantic University, Ocean Engineering Department, Boca Raton, FL 33431, USA

ARTICLE INFO

Article history:
Received 17 October 2008
Received in revised form
13 February 2010
Accepted 19 February 2010
Handling Editor: P. Joseph
Available online 7 April 2010

ABSTRACT

Leading edge noise measurements and calculations have been made on a three airfoils immersed in turbulence. The airfoils included variations in chord, thickness and camber and the measurements encompass integral scale to chord ratios from 9 to 40 percent as well as 4:1 ratios of leading edge radius and airfoil thickness to integral scale. Angle of attack is found to have a strong effect on the airfoil response function but for the most part only a small effect on leading edge noise because of the averaging effect of the isotropic turbulence spectrum. Angle of attack effects can therefore be significant in non-isotropic turbulence and dependent on airfoil shape. It is found that thicker airfoils generate significantly less noise at high frequencies but that this effect is not determined solely by the leading edge radius or overall thickness. Camber effects appear likely to be small. Angle of attack effects on the response function of a strongly cambered airfoil are shown to be centered on zero angle of attack, rather than the zero lift angle of attack.

1. Introduction

The interaction of a turbulent flow with a lifting surface is an important source of sound in many situations including aircraft engines, submarine propellers and wind turbines. Wakes shed by the aircraft engine fan blades convect downstream and interact with following stator blades or vanes. Turbulence encountered by a submarine propeller is created by the vehicle boundary layer and flows over inlet guide vanes. Turbulence from the atmospheric boundary layer and upstream obstructions is encountered by the blades of a wind turbine. In all these situations, broadband noise is generated, which can be a significant portion of the overall noise.

At low Mach numbers this noise originates from the unsteady pressure field produced by the airfoil in response to the turbulence. These pressure fluctuations are primarily generated by the impact of the turbulence upon the impenetrable surface of the airfoil, and it is the portion of this that radiates to the far field which we hear as sound. Sound radiation from blades encountering a turbulent flow has been studied extensively for many years, one product of which is a large body of theoretical work and associated prediction methods (see reviews by Mish and Devenport [1] and Glegg and Devenport [2]). These theoretical developments have been based on a somewhat smaller set of experimental studies, a number of which have focused on observations at one or two disturbance wavenumbers (e.g. Commerford and Carta [3], Manwaring and Fleeter [4]), on airfoils embedded in inhomogeneous turbulence (e.g. Sharland [5], Olsen and Wagner [6]), or in applied situations (e.g. Aravamudam and Harris [7]) where confounding factors can be hard to separate. The number of

* Corresponding author. Tel.: +1 540 231 4456; fax: +1 540 231 9632.
E-mail address: devenport@vt.edu (W.J. Devenport).

0022-460X/$ - see front matter © 2010 Elsevier Ltd. All rights reserved.
doi:10.1016/j.jsv.2010.02.022

experimental studies where the response and/or noise of simple airfoil geometries embedded in homogeneous turbulence is comparatively small.

Perhaps the best know experimental study of leading edge noise and response is due to Paterson and Amiet [8]. They investigated the far-field noise and unsteady surface pressure field of a NACA 0012 airfoil operating downstream of a bi-planar turbulence grid. The testing was performed in an open-jet anechoic wind tunnel. Two-point two-component velocity fluctuation measurements were made to demonstrate the homogeneity and isotropy of the turbulence which was found to have an integral scale equivalent to 13 percent of the airfoil chord and a turbulence intensity of about 4 percent. They studied, primarily, the behavior of the airfoil at zero angle of attack and found surface pressure fluctuations and far-field sound to be reasonably well predicted by their own inviscid flat-plate response theory. One exception here is the far-field sound at high frequencies which was found to fall below the predictions by about 5 dB. They attribute this to the finite airfoil thickness, an assertion quantitatively verified by Gershfeld [9]. Some measurements at 8° angle of attack are discussed (but not presented). Patterson and Amiet [8] report seeing a slight increase in sound pressure levels (<2 dB) with angle of attack that is independent of observer angle or speed.

Real airfoil effects (of angle of attack and thickness) are apparent in the more recent studies of Oerlemans and Migliore [10] and Moreau et al. [11]. Oerlemans and Migliore studied the leading edge noise generated by six airfoils designed for use on small wind turbines (an S822, S834, FX63-167, SG 6043, SH3055 and SD2030). They immersed the airfoils in turbulence generated by a grid placed in the settling chamber of the wind tunnel. The turbulence was rapidly decaying, varying from 11 percent turbulence intensity at the leading edge location to 6 percent at the trailing edge. Integral scale was not measured but might be expected to have been about 8 percent chord. The airfoils were placed in the open-jet test section of their facility and corrections (of about -56 percent) made for the impact of interference on the effective angles of attack of their airfoils. Far-field sound was recorded using a phased array at a distance of 0.6 m from the airfoils. They observed that an increase in the effective angle of attack from 0 to 7.9° increased far-field noise levels by between 1 and 3 dB at reduced frequencies ω_r (based on semichord) between 15 and 45. By comparing measurements made with the different airfoils, they observed general trend of reduction of noise levels by about 7–10 dB with increase in thickness (interpreted as leading edge radius) over this frequency range.

Moreau et al. [11] used a somewhat similar arrangement to study the leading edge noise generated by grid turbulence interacting with three different bodies: a flat plate with 3 percent thickness, a cambered controlled diffusion airfoil of 4 percent thickness, and a NACA 0012 airfoil. They too generated turbulence using a grid placed in the settling chamber of their open-jet tunnel, and used single component hot-wire measurements to verify homogeneity and establish the turbulence intensity to be 5 percent and the integral scale to be equivalent to 9 percent of the chord of the 0012 and flat plate, and 7 percent of the chord of the controlled diffusion airfoil. They studied the effects of geometric angle of attack between 0° and 15°. Effective angles of attack (accounting for a 64 percent correction implied by their test section geometry) would have ranged between 0° and 5.4°. Their NACA 0012 measurements show little effect of angle of attack and they conclude that angle of attack plays no significant role in the far-field noise within this range. They observe thickness to have a substantial effect on noise levels for $\omega_r > 4$ with the NACA 0012 producing noise levels about 10 dB quieter than the other two foils in this range. They interpret this effect as occurring when the thickness exceeds the integral scale. Patterson and Amiet [8] argue that the effect should appear when the circular frequency, normalized using the leading edge thickness and flow velocity, exceeds 1. These criteria are equivalent in Moreau et al.'s experiment.

Effects of angle of attack can be seen in the leading-edge response studies of McKeough and Graham [12] and Mish and Devenport [1,13]. These researchers did not measure radiated sound and used closed test section tunnels. McKeough and Graham [12] made experimental measurements to verify their theoretical results on a NACA 0015 airfoil placed in grid generated turbulence. They measured the *overall* unsteady lift on the airfoil using three piezo-electric transducers connected to the airfoil. Measurements were made for incidence angles of $\alpha=0^\circ$ and 10° and for two turbulence grids producing turbulence scale of $\Lambda/c=0.4$ and 0.38 and turbulence intensities of 5.8 and 3.7 percent, respectively. Their results show that the admittance function $|A(\omega)|^2$, defined as the ratio of the lift spectrum to the turbulence upwash spectrum, increases by approximately 3 dB as the angle of attack is increased for $\omega_r < 1$. Mish and Devenport [1,13] studied the effect of grid generated turbulence on a NACA 0015 airfoil. Two-point three-component measurements showed a closely isotropic homogeneous flow with an integral scale of 13 percent of the chord and a turbulence intensity of 4 percent. Measurements were performed at angles of attack from 0° to 20°, interference corrections in their closed tunnel being only a few percent. They used an array of surface mounted microphones to measure surface pressure correlations and lengthscales and integrated these to obtain *sectional* lift spectra. (The sectional lift spectrum would differ from the total lift spectrum by a spanwise correlation lengthscale dependent on frequency.) Mish and Devenport's spectra show a reduction in the unsteady sectional lift of about 5 dB with increasing angle of attack for $\omega_r > 5$. They also observe that the departure of the mean square lift from its zero angle of attack value varies as the square of the angle of attack—a result first predicted by McKeough and Graham [12].

One reason why the above cited experimental studies paint a rather disparate picture of real airfoil effects, particularly of angle of attack, is that these effects are not easy to measure. Far-field sound measurements are usually only possible in an acoustically open test section and free jet airfoil flows require large angle of attack corrections. These corrections imply substantial deflection of the jet, and thus distortion of the oncoming turbulence that is not present in free flight. Furthermore, turbulence generating grids tend to be noisy and thus are often placed in the settling chamber to prevent

contamination. This leads to additional distortion of the onset turbulence. These problems can be overcome by using a closed test section, but then one is restricted to inconclusive near-field studies.

In the experimental part of this study we have attempted to overcome these problems. We have used a novel anechoic facility with acoustically transparent Kevlar test section walls. The walls contain most of the flow and greatly reduce flow deflection and lift interference. We have used the same homogeneous isotropic grid turbulence as Mish and Devenport [1], and studied the noise radiated by three airfoils of varying chord, leading edge radius and camber as functions of angle of attack. Noise measurements have been compared with absolute sound predictions made using a panel method calculation, and the theory of Glegg and Devenport [2]. The calculations also provide insight into the physics behind the effects observed experimentally.

2. Apparatus and instrumentation

2.1. Wind tunnel

Tests were performed in the Virginia Tech Stability Wind Tunnel. This facility is a continuous, single return, subsonic wind tunnel with 7.3 m long removable rectangular test sections of square cross section 1.83 m on edge. Flow through the empty test section is closely uniform and has a streamwise turbulence intensity of 0.02 percent at 30 m/s (Choi and Simpson [14], Remillieux et al. [15]). The Stability Wind Tunnel is unique in that it has an anechoic system that can be installed or removed at will. The anechoic system consists of an acoustic test section flanked by two anechoic chambers (Fig. 1). The test section consists of upper and lower walls that run the full 7.3 m length of the test section, treated to reduce or eliminate acoustic reflections, and partial side walls, also treated, at the test section entrance and exit. Rectangular openings in the side walls, which extend 4.2 m in the streamwise direction and cover the full 1.83 m height of the test section, serve as acoustic windows. Sound generated in the flow exits the test section through these into the anechoic chambers to either side. Large tensioned panels of Kevlar cloth cover the openings permitting the sound to pass while containing the bulk of the flow. The test section arrangement thus simulates a half-open jet, acoustically speaking. The Kevlar windows eliminate the need for a jet catcher and, by containing the flow, substantially reduce the lift interference when airfoil models are placed in the test flow. This arrangement is a relatively recent innovation. Further details of the system and its calibration are given by Staubs [16], Crede [17] and Remillieux et al. [15].

The Kevlar cloth forming the acoustic windows is stretched on a 5.37×2.51 m tensioning frame to a tension of the order of 1500 Newtons per linear meter. The Kevlar windows are sewn from three lengths of Kevlar cloth. When mounted the

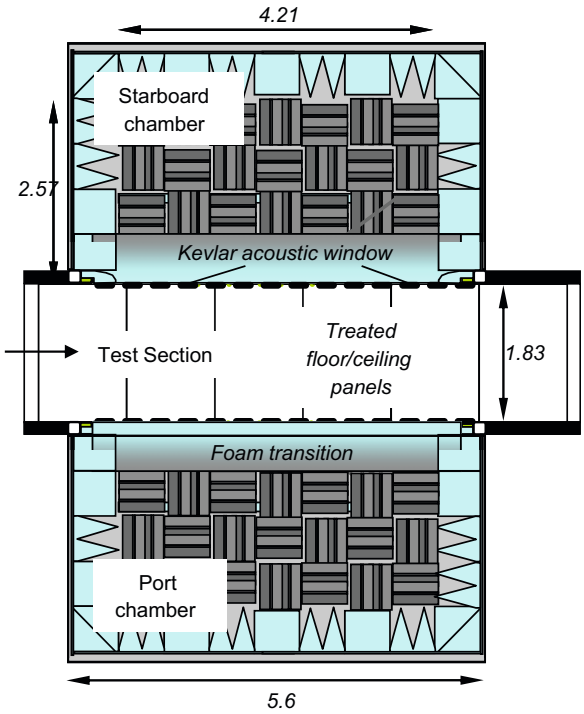

Fig. 1. Plan view cross-section of the anechoic system as installed showing the test section flanked by the two anechoic chambers. Dimensions in meters. Black shaded areas of the test section side walls are acoustically treated.

two 40 mm-wide seams run streamwise along the test section 0.19–0.28 m below the upper wall and a similar distance above the lower wall.

The two anechoic chambers are positioned on either side of the test section (Fig. 1). Each chamber has a streamwise length of 6 m, extends 2.8 m out from the test section acoustic window, and has a depth of 4.2 m. The chambers are lined with 0.610 m high acoustic foam wedges designed to eliminate acoustic reflections at frequencies above 140 Hz. Quarter-elliptical foam sections surround the acoustic windows so as to form a smooth transition between the lower and upper walls of the test section, on the inside of the windows, and the acoustically treated walls of the anechoic chambers on the outside of the acoustic windows. The chamber sections are designed to seal to the sides of the test section, so as to minimize any net flow through either acoustic window.

2.2. Turbulence grid

The same grid employed by Mish and Devenport [1] was used for this study. This is a biplanar grid of 5 by 2.5 cm rectangular bars mounted on 30 cm centers giving an open area ratio of 69.4 percent. The 10 cm high acoustic foam wedges are glued to the downstream face of the bars to provide some attenuation of the grid noise. The grid was mounted in the wind tunnel contraction at a point where the cross sectional area is 32 percent larger than that of the test section, this position being about 19.5 mesh sizes upstream of the test airfoils. This position was chosen so that the remaining portion of the contraction would be just sufficient to isotropize the slightly compressed turbulence otherwise produced by the grid, see Bereketab et al. [18], and so that streamwise decay over the length of the airfoils would be small. Note that this grid was chosen for compatibility with Mish and Devenport, but also as the result of a study of different grid configurations, the turbulence levels and noise they produce. The rectangular bar grid was found to be quieter and generate higher turbulence levels than a series of similarly mounted circular-bar grid configurations, see Staubs [16].

Bereketab et al. [18] present detailed single and two-point three-component turbulence measurements made in a cross section through the flow at the test airfoil location for a flow speed of 30 m/s. They show the rectangular-bar grid to generate closely homogenous and isotropic turbulence, with turbulence intensities in the three orthogonal directions differing by <5 percent. Longitudinal and lateral turbulence spectra and spatial correlations conform closely to a von Karman spectrum with a longitudinal integral scale L of 82 mm and a turbulence intensity of 3.9 percent. Fig. 2 compares time spectra (measured at two distinct sampling rates) and two point correlations (measured explicitly in the spanwise and lateral directions and inferred using Taylor's hypothesis in the streamwise direction) with the von Karman model. Dissipation estimates derived from these data indicate a rate of decay that would result in about a 4 percent reduction in turbulence levels per meter of streamwise distance.

2.3. Airfoil models

Three airfoil models of varying chordlength and section are considered. All were designed to span the complete 1.83 m height of the test section. Fig. 3 compares the sectional shape and size of the different models and shows them relative to the turbulence integral scale. Table 1 quantitatively summarizes this information, and other airfoil properties. The airfoil models were the result of a range of fabrication methods. The NACA 0012 airfoil was made in-house from solid aluminum stock using a CNC machine. The NACA 0015 airfoil (the same model used by Mish and Devenport [1,13]) was also fabricated in-house but from an extruded aluminum section. The S831 model was constructed by Novakinetics LLC with a fiberglass composite skin and a fill of fiberboard and polyurethane foam.

During testing the airfoil models were mounted vertically in the test section with the quarter chord line 3.56 m downstream of the test section entrance and perpendicular to the oncoming flow. Small residual gaps between the ends of the model and the upper and lower test section walls were covered and faired using aluminum foil tape. Models were rotated to angle of attack about the quarter chord location and were instrumented with pressure taps so that the effective angle of attack could be determined aerodynamically. A boundary layer trip, fabricated from metal tape cut with pinking shears so as to have a serrated edge placed at the 10.7 percent chord location, was used with the NACA 0012. No boundary layer trips were used on the other airfoils.

2.4. Microphones

Half-inch Type 4190 Bruel and Kjaer microphones were used. These have a nominal sensitivity of 50 mV/Pa and a flat frequency response up to 20 kHz. For the measurements presented in this paper two or four of these microphones were mounted in the anechoic chambers 1.8 m from the airfoil leading edge at mid-span in the direction of positive mean lift (i.e. an observer angle of 0° measured about the leading edge line). The microphones were oriented so as to face the leading edge, and be normal to the incident flow direction. When using two microphones they were separated by a short distance in the streamwise direction (0.15 m). When using four they were separated by 0.15 m in the streamwise and spanwise directions. In both cases the center of the microphone group was set at the observer angle of 0°. Sound spectra were obtained from the average of the multiple microphone signals to reduce sensitivity to background noise sources far upstream or downstream of the airfoils. The microphones were used in conjunction with a B&K Nexus 2690 amplifier using

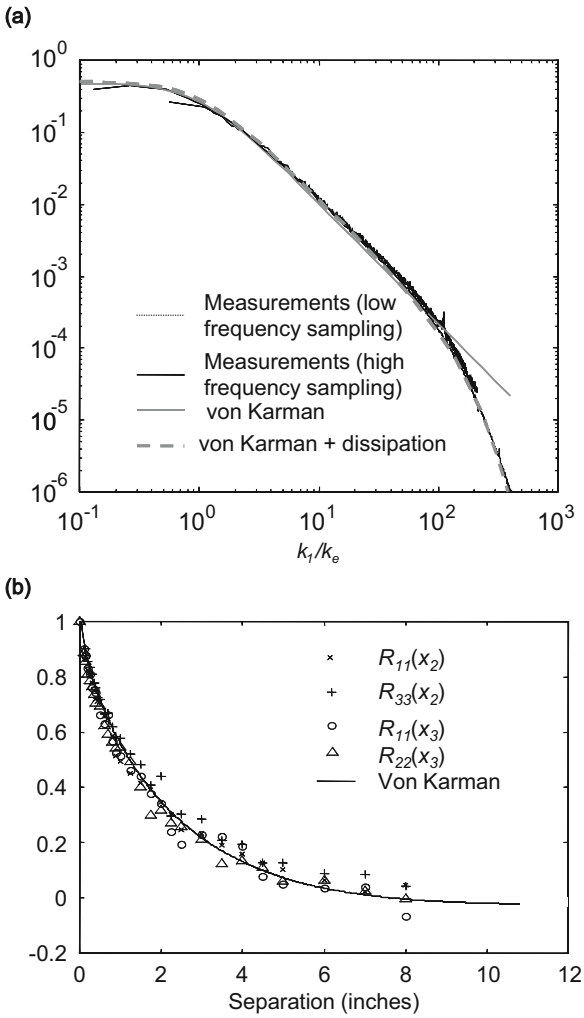

Fig. 2. (a) Non-dimensional streamwise velocity autospectra and (b) lateral correlation functions 19 mesh sizes downstream of the turbulence grid with no airfoil present compared to the von Karman interpolation formula for a turbulence intensity of 3.9 percent and an integral scale of 82 mm, from Bereketab et al. [18].

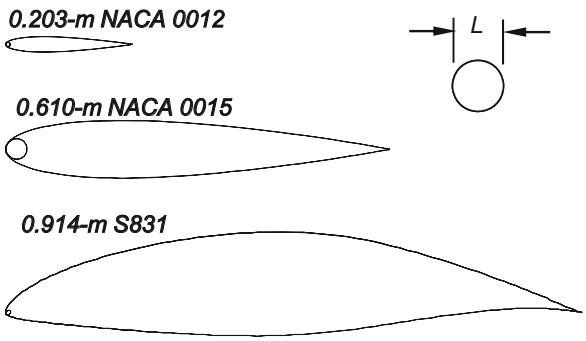

Fig. 3. Airfoil shapes and sizes compared with the turbulence longitudinal integral scale *L*. The small circles illustrate the leading edge radii.

the nominal sensitivity provided by the manufacturer. Sensitivity was checked using a B&K model 4228 Pistonphone and was found to vary only ± 1 percent from the nominal value. Microphone outputs were measured simultaneously using an Agilent E1432 16-bit digitizer. Spectra presented here are the result of a combination of two sampling schemes. Low frequency (<600 Hz) resolution was obtained by averaging 250 records of 1600 samples recorded at 1600 Hz for each

Table 1
Airfoil characteristics.

Airfoil	Chordlength c (mm)	Thickness t (mm)	Leading edge radius r_{le} (mm)	L/c	L/t	L/r_{le}	Zero lift angle of attack α_0 (deg)
NACA 0012	203	25.4	3.6	0.403	3.22	23.0	0
NACA 0015	610	91.4	16.3	0.134	0.89	5.0	0
S831	914	165.1	3.8	0.089	0.5	21.5	−7

condition, while high frequency (>600 Hz) resolution was obtained by averaging 250 records of 8192 samples recorded at 51 200 Hz.

3. Calculations

Predictions of absolute sound levels generated were performed using an incompressible vortex panel method and the theory described by Glegg and Devenport [2]. These calculations assume an acoustically compact airfoil for which the noise spectrum heard by an observer at an angle θ and a distance r from the airfoil $S_{pp}(\omega)$ is related to the unsteady lift spectrum $S_{LL}(\omega)$ as

$$S_{pp}(\omega)=\left(\frac{\omega\cos\theta}{4\pi r c_0}\right)^2 S_{LL}(\omega) \tag{1}$$

where c_0 is the sound speed and ω the angular frequency. As shown by Glegg and Devenport [2] the unsteady lift spectrum produced by the incident 3-D turbulence can be determined entirely from the spanwise vorticity and the 2-D airfoil response function as

$$S_{LL}(\omega)=\frac{4\pi R_3}{U_\infty}\int_{-\infty}^{\infty}\Omega_{33}(k_0,k_2,0)\,|S(k_0,k_2,0)|^2\,\mathrm{d}k_2 \tag{2}$$

where R_3 is the airfoil half-span, Ω_{33} the spanwise-vorticity wavenumber spectrum of the incident turbulence, $k_0=-\omega/U_\infty$, k_2 is wavenumber in the direction of mean lift, and $S(k_0,k_2,0)$ is the 2-D wavenumber frequency response function of the airfoil lift, per unit span. For homogeneous turbulence, $\Omega_{33}(k_0,\,k_2,\,0)=E(k)/4\pi$, where $k=(k_0^2+k_2^2)^{1/2}$ and $E(k)$ is the 3-D velocity energy spectrum. Eq. (1) only applies when the airfoil can be considered acoustically compact, which requires that differences in propagation distance from points on the airfoil to the observer are small compared to the acoustic wavelength. In the experimental results presented here the measurements were made using a microphone at 90° to the airfoil surface and the differences in propagation distance are less than $c^2/8r$. The measurements were limited to frequencies below 1000 Hz and so the compactness condition which requires $c^2/8r\lambda\ll 1$ is met for all conditions and airfoils considered.

As discussed by Glegg and Devenport [2], $S(k_0,k_2,0)$ is the 2-D integrated lift response function of the airfoil which depends on the frequency ω of the incoming disturbance and its wavenumber in the direction of lift k_2. This function is the Fourier transform of the linear time response of the lift to an elemental vortex of unit strength released infinitely far upstream of the airfoil, i.e.

$$S(k_0,k_2,0)=\frac{2\pi U_\infty}{2R_3\Gamma}\int_{-\infty}^{\infty}\int_{-\infty}^{\infty}L_v(t,x_2)\mathrm{e}^{\mathrm{i}\omega t-\mathrm{i}k_2x_2}\,\mathrm{d}x_2\,\mathrm{d}t \tag{3}$$

The position x_2 is the initial distance, measured in the direction of lift, from the stagnation streamline to the vortex. The panel method is used to obtain this time response function $L_v(t,x_2)$ through a complete representation of the airfoil and wake geometry. Each airfoil was represented using a total of 200 panels with lengths varying from 0.1 percent c at the trailing edge to 3.2 percent c near mid-chord to 0.1 percent at the leading edge. Incident vortices were released 10 chords upstream of the leading edge and allowed to convect over a total time period of $20U_\infty/c$ in even time steps of $0.01U_\infty/c$. The unsteady loading for 100 different initial incident vortex locations, from $x_2=-5c$ to $5c$, was computed. Locations in x_2 were not evenly spaced but concentrated around the stagnation streamline in a parabolic distribution, with the smallest positive and negative x_2 locations being $\pm 0.002c$. The Fourier transform of Eq. (3) required an interpolation in x_2 (in steps of 0.01) and windowing in time and x_2 (Chebyshev). As discussed by Glegg and Devenport [2] results were found to be converged and independent of these choices and accurate up to a reduced frequency of about 40.

Fig. 4 illustrates the response function for the NACA 0015 airfoil at 8° angle of attack. In Fig. 4a L_v is plotted vs. time t and initial disturbance position x_2 (effectively the drift coordinates). In Fig. 4b it is plotted in terms of the physical coordinates y_1 and y_2 representing the actual position of the vortex relative to the airfoil when the response is produced.

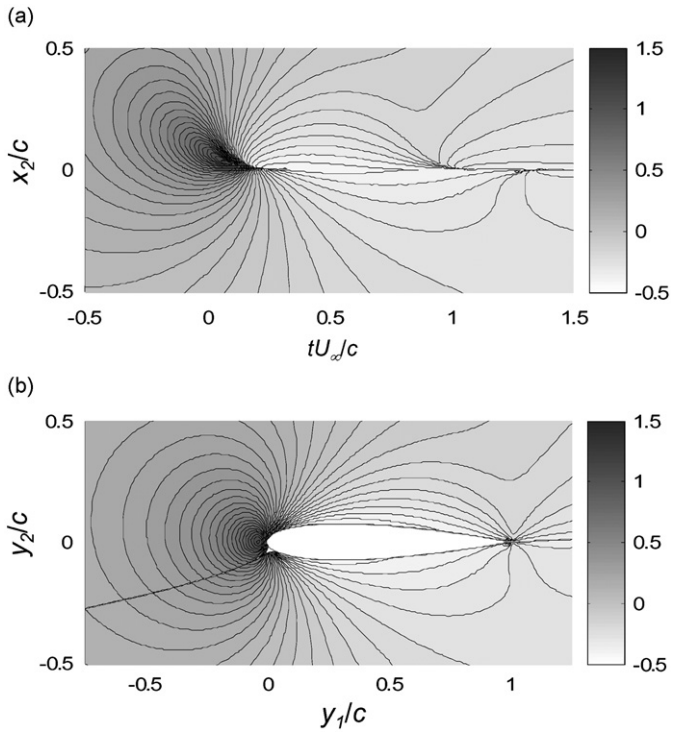

Fig. 4. Response function for the NACA 0015 airfoil at 8° angle of attack (a) in physical coordinates and (b) in drift coordinates.

Not surprisingly the airfoil is most sensitive to vorticity convected through the space just upstream of its leading edge. In this position the airfoil blocks almost the entire upwash associated with the vorticity hence the strong lift response. The response actually reaches its maximum just ahead of the leading edge, rather than on its surface, because of the finite leading edge radius. Essentially the effects of vorticity approaching very close to the leading edge are cancelled by its image in the airfoil surface. Also the airfoil produces no significant response to vorticity near its trailing edge because of the canceling effect of vorticity shed into the airfoil wake as a consequence of the Kutta condition. Shown in terms of drift coordinates (Fig. 4a) we see the effect that the flow distortion around the leading edge has on the timing of the response. In this specific case, the response maximum ahead of the leading edge is entirely accessed by vorticity that originates above the stagnation streamline, and thus, in terms of drift coordinates, this region appears entirely in the positive x_2 half-plane. Furthermore, it is skewed by the different convection speeds associated with vorticity different distances from the stagnation streamline.

The lift response function calculations were based on incompressible flow theory and neglect the effect of compressibility on the blade response. This assumption is known to be in error at high frequencies [19] when the blade chord exceeds a quarter of the acoustic wavelength. Calculations using the high frequency compressible solutions given by Amiet [19] show that at Mach number of the flow in this experiment (M=0.08) the incompressible and compressible solutions are almost identical up to reduced frequencies of 16, which is close to the upper limiting frequency where signal to noise problems affect the measured data in this experiment.

4. Results and discussion

4.1. The NACA foils

All measurements presented in this paper were made for a free-stream velocity of 30 ± 0.5 m/s, corresponding to a Reynolds number per meter of 1.8 million. Measured sound spectra were post-processed to eliminate background contamination. Fig. 5 shows raw spectra measured at the same test speed for various configurations involving the NACA0012 airfoil. Except at very low frequencies, the lowest sound levels are recorded with the empty test section, with no airfoil or grid installed. Adding only the NACA0012 airfoil makes little difference to the levels except between about 200 and 800 Hz where small increases are seen, possibly as a result of trailing edge noise or noise generated by the junctions between the ends of the airfoil model and the wind tunnel floor and ceiling boundary layers. Changing the angle of attack of the airfoil has little impact on this background noise level. Removing the airfoil and adding the turbulence grid produces a large jump in noise levels. At high frequencies ($>$ 800 Hz) this increase is broadband and is believed to result from an

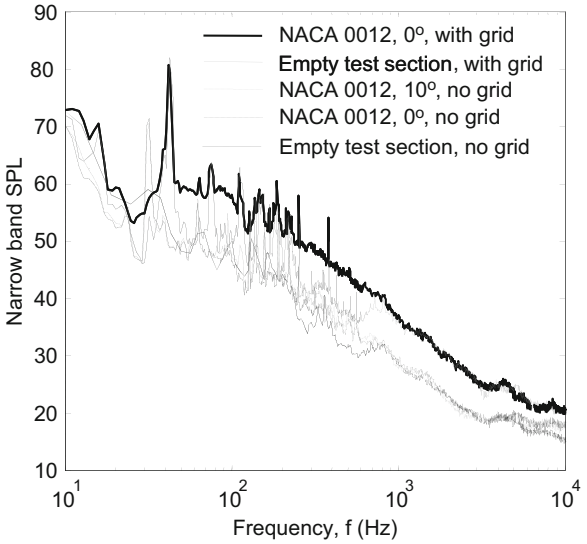

Fig. 5. Raw sound spectra measured with the NACA 0012 airfoil for various test section conditions.

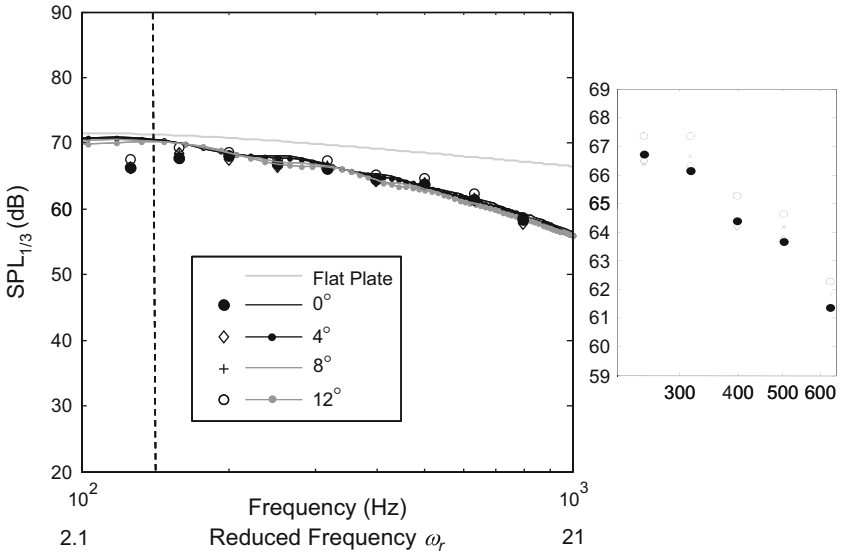

Fig. 6. NACA 0012 airfoil. Leading edge noise as a function of angle of attack. Lines show panel method predictions. Inset figure shows expanded SPL scale. Chamber not expected to be anechoic below 140 Hz.

increase in noise from the wind tunnel fan, a consequence of the higher speed needed to overcome the drag of the grid. At lower frequencies the increase is mostly in tones apparently generated by the grid bars themselves, as illustrated in Fig. 5. Re-installing the airfoil with the grid present adds leading edge noise to the spectrum. No discernable noise is generated above 1 kHz, but below this frequency the leading edge noise appears consistently 7–10 dB above the grid noise background except where strong tones are present.

Grid associated noise was observed to be the dominant contributor to background noise levels for the larger airfoils as well. Leading edge noise spectra were therefore obtained by subtracting background noise levels, obtained with only the grid installed, from those measured with airfoil and grid. Because of the narrow-band nature of the grid noise, measurements at frequencies below 600 Hz were made with a 1 Hz bandwidth and particular care was taken to match flow speeds and thus the peak frequencies. Data were discarded in 1 Hz bands where the signal to noise ratio was < 3 dB. If this resulted in a gap in the spectrum, interpolation was used over the gap so that 1/3rd octave bands could still be integrated.

Fig. 6 shows leading edge noise spectra for the small (0.20 m chord) NACA 0012 airfoil for 0°, 4°, 8° and 12° presented as a function of angle of attack in 1/3rd octave band SPL. Measurements are presented between 100 and 1000 Hz, corresponding to reduced frequencies between 2.1 and 21. Note that the chambers are not expected to be fully anechoic

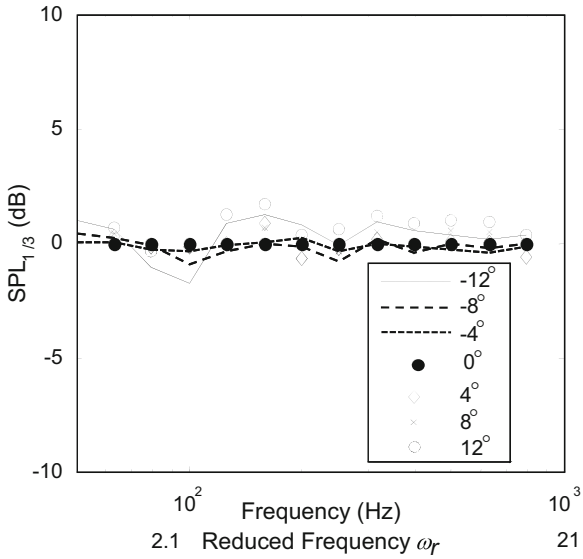

Fig. 7. NACA 0012 airfoil. Leading edge noise levels relative to zero angle of attack.

below 140 Hz and this frequency is denoted by the vertical dashed line. The sound spectra have a broad form with peak levels of about 70 dB. Angle of attack effects are small. Spectral levels change very little between 0° and 8°. Between 8° and 12° there is a slight increase that appears to be almost uniform across the frequency range, but the total angle of attack effect appears to be no more than about 1 dB. Spectra can be compared with results from the predictions, shown for a flat plate at zero angle of attack and for the full airfoil geometry at all measured conditions. Overall, the full predictions agree well with the measurements, the discrepancies being everywhere < 2 dB. Consistent with the experiment, the predictions show almost no angle of attack effect. Comparing with the flat-plate prediction we see that noise levels at high frequencies are severely attenuated by the airfoil thickness, even though the airfoil thickness and leading edge radius are less than 1/3rd and 1/20th, respectively, of the turbulence integral scale. The thickness effect starts to become apparent at a reduced frequency of about 3, corresponding to a circular frequency normalized on airfoil thickness and free stream velocity of about 0.12, considerably less than the value of 1 suggested by Patterson and Amiet [8].

Significant leading edge noise was generated by the airfoil below the anechoic limit of the wind tunnel. While absolute levels probably cannot be relied on in this region, the relative changes on sound level with angle of attack should be correctly measured although it is an open question whether they are representative of the acoustic far field. Fig. 7 shows these relative changes down to an absolute frequency of 50 Hz or a reduced frequency of 1.1. If anything, effects of angle of attack appear even smaller in this low frequency range. This plot also compares measurements made at positive and negative angles of attack. The effects of angle of attack appear symmetric to within better than 1 dB with a significant increase in sound levels at negative angle of attack only occurring between $-8°$ and $-12°$.

Fig. 8 shows leading edge noise measurements and calculations for the 0.61 m NACA 0015 airfoil. At zero angle of attack this airfoil, which is three times the chord and over 3.6 times the thickness of the small 0012, produces much less noise at higher frequencies with little being detectable above 300 Hz (ω_r=19.2). We therefore see less of the spectrum and greater uncertainty at some frequencies. Nevertheless, it is clear that the angle of attack effects for the NACA 0015 are still small and, at all frequencies sound levels increase by about 2 dB as the angle of attack is increased to 12°. Again there is a good correlation between experiment and prediction, at least up to a frequency of about 500 Hz where it is possible that uncertainty in the background noise subtraction is significantly influencing the plotted values. The predictions show a slight increase in noise levels with angle of attack (about 2 dB at 400 Hz) that is greater at high frequencies.

4.2. Understanding real airfoil effects

The small effect of angle of attack on leading edge noise from the two NACA foils is consistent with Patterson and Amiet's [8] and Moreau et al.'s [11] observations, and might reasonably be taken as evidence that the response functions of these airfoils is also almost constant with angle of attack. However, this is not the case. Fig. 9 compares the calculated response function in wavenumber–frequency space $S(k_0,k_2,0)$ for the NACA 0015 airfoil at 0° and 8° (plots for the 0012 airfoil are very similar). At 0° angle of attack the response function has a maximum near the origin and a surrounding decay that is symmetric in k_2. The response is symmetric in k_2 because in physical space it is symmetric about the stagnation streamline. However, as the angle of attack is increased, the stagnation streamline shifts to the pressure side of the airfoil

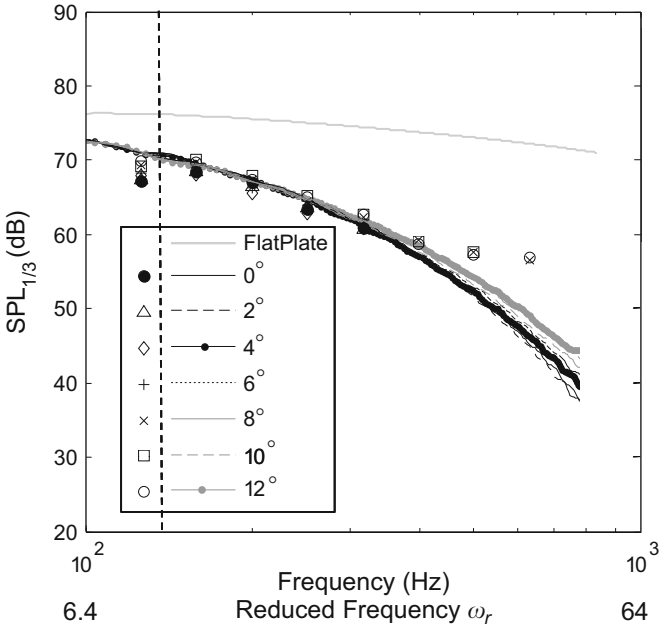

Fig. 8. NACA 0015 airfoil. Leading edge noise levels. Points indicate measurements, lines are predictions.

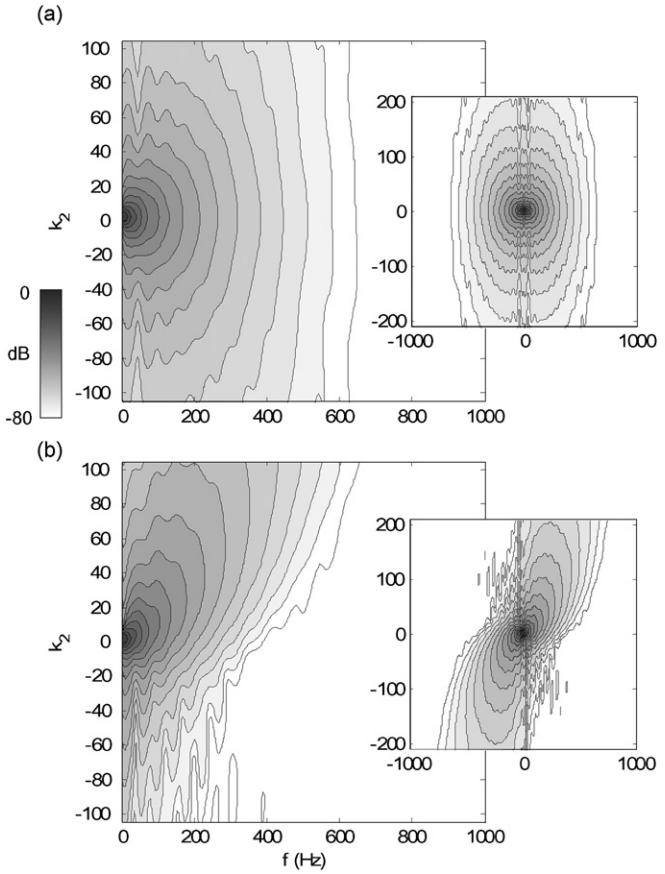

Fig. 9. Response functions in wavenumber frequency space for the NACA 0015 airfoil at (a) 0° and (b) 8° angle of attack in dB relative to maximum value. The function shown in (b) is the 2-D Fourier transform of Fig. 4a.

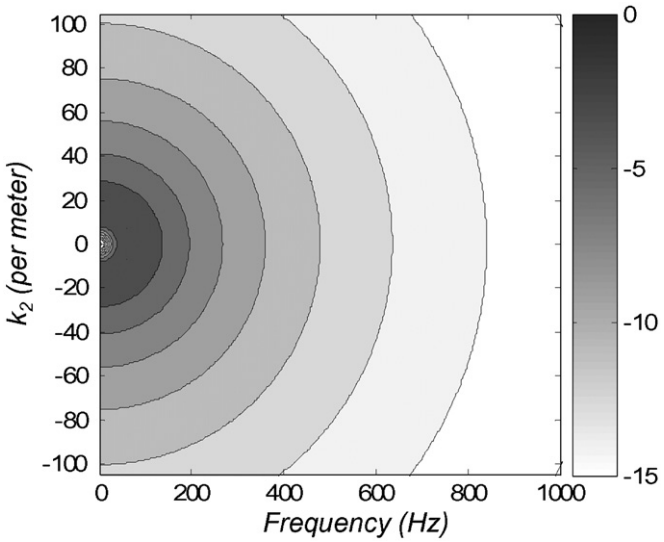

Fig. 10. Spanwise vorticity spectrum implied by the von-Karman formula for an integral scale 82 mm in dB relative to maximum value.

(as in Fig. 4b). The response function thus becomes heavily skewed with angle of attack, both in terms of drift coordinate x_2 and wavenumber k_2.

The weak influence of angle of attack on the sound spectrum can therefore only be explained in terms of the multiplication of the response function by the isotropic turbulence spectrum (Fig. 10) and the averaging in k_2 that takes place in Eq. (2). In other words, the upward shift of the response function in Fig. 9 must occur in such a way as to not significantly change its average product with the circular contours of turbulent vorticity spectrum in Fig. 10. This seems likely to be a result of this particular spectrum and response function. We therefore hypothesize that with a significantly different inflow turbulence spectrum or different airfoil geometry significant angle of attack effects would be seen in the sound spectrum.

We can test the first of these hypotheses by considering the sound radiated by the NACA 0015 airfoil in the case of anisotropic turbulence. We use the axisymmetric turbulence model of Kerschen and Gliebe [20,21] which assumes that the turbulence has different lengthscales in the streamwise and lateral directions l_a and l_t. They provide analytical expressions for the velocity spectrum tensor $\Phi_{ij}(\boldsymbol{k})$ is easily related to the vorticity spectrum tensor $\Omega_{ij}(\boldsymbol{k})$ (see Batchelor [22]), to give

$$\Omega_{33}(k_0,k_2) = \frac{2l_a l_t^4 u_a^2 k^4}{\pi^2[1+l_a^2k_0^2+l_t^2k_2^2]^3} \tag{4}$$

where u_a is the turbulence intensity in the streamwise direction. Setting l_a and l_t equal to each other and the turbulence integral scale produces an isotropic vorticity spectrum and sound predictions almost identical to those obtained with the von Karman interpolation used above. What is interesting is the sound predictions obtained with the same model but for the anisotropic turbulence spectrum obtained by setting l_t=0.5 l_a, as shown in Fig. 11. The sound is seen to rise quite rapidly with angle of attack in the anisotropic turbulence, by 5–10 dB between 0° and 12°. The implication is that wind tunnel grid-turbulence studies and isotropic turbulence calculations may significantly underestimate angle of attack effects seen in practical applications where anisotropic inflow turbulence is common.

The second hypothesis can be examined by considering calculations and some measurements of the sound generated by the 0.91 m chord S831 airfoil. This presents an interesting contrast to the NACA airfoils. Despite being 4.5 times the chord of the NACA 0012 it has almost the same leading edge radius (Table 1). At the same time it is almost twice as thick as the NACA 0015 and heavily cambered with a zero lift angle of attack of $-7°$. Sound measurements and calculations are presented in Fig. 12. Unfortunately the mean aerodynamics of this foil were not ideal. For angles of attack of 0–2°, aerodynamic measurements indicated the presence of some suction-side stall downstream of mid-chord (Devenport et al. [23]). Above about 2° surface pressure measurements indicate the presence of additional viscous effects downstream of the suction side leading edge, progressing to complete stall at about 8°. Measurements are therefore only presented for 0° and 2°. These measurements show good agreement with calculations at low frequencies ($\omega_r < 16$) where the effects of compressibility in the measurements would have been small. At higher frequencies the measured sound levels, as far as they are audible, remain consistent with the predictions even though these neglect compressibility effects.

In and of themselves the predictions are still meaningful at high frequencies. They just reflect effects that would be seen at a lower Mach number than the measurements. Comparing the three sets of calculations (Figs. 6, 8 and 12) we see that

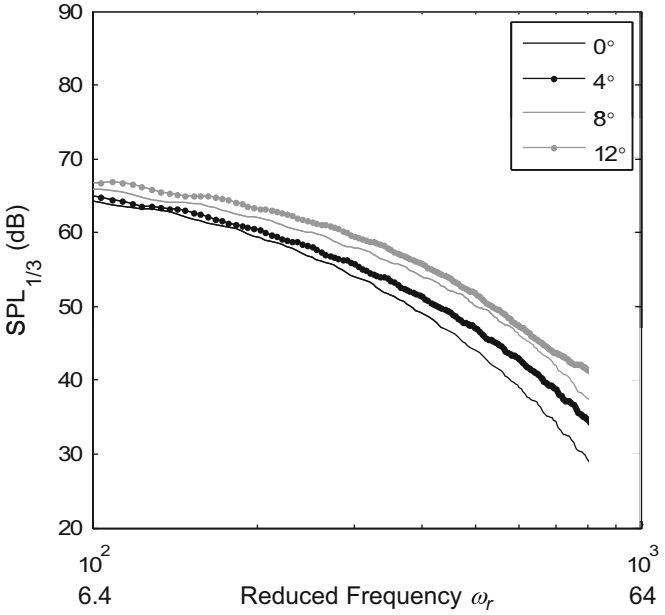

Fig. 11. Leading edge noise levels predicted for the NACA 0015 airfoil with anisotropic inflow turbulence with a lateral lengthscale equal to half the streamwise lengthscale.

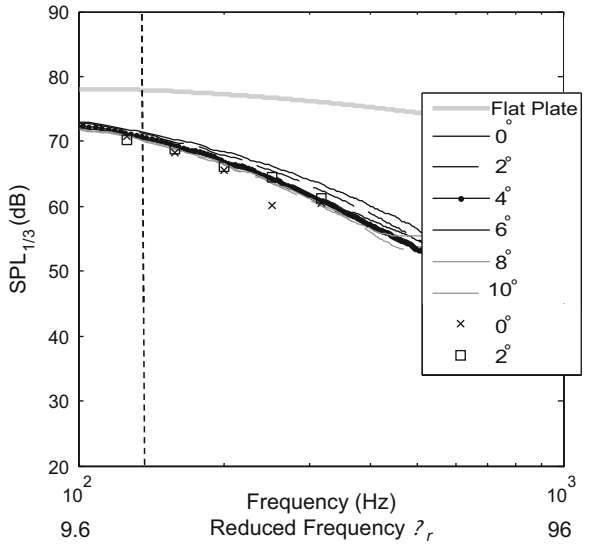

Fig. 12. S831 airfoil. Leading edge noise levels. Points indicate measurements, lines are predictions.

the S831 produces noticeably less sound at higher frequencies than the NACA 0012 despite the similar leading edge radius but more sound than the NACA 0015 despite the larger overall thickness. This highlights the complexity of the thickness effect which, at least in this case, is clearly not a unique function of either of these parameters. Furthermore, the sound generated by the S831 is clearly a function of angle of attack, decreasing by about 4 dB between 0° and 4°. This behavior is markedly different than that seen with the NACA 0012 or NACA 0015 and tends to confirm our hypothesis that angle of attack effects are a function of airfoil geometry.

A particularly interesting feature of this behavior is the fact that the angle of attack effects on the response function of this airfoil are centered on zero angle of attack, rather than the zero-lift angle of attack (a 7° difference). As shown in Fig. 13 the response function is almost symmetric at zero angle of attack with increases and decreases in angle of attack from this position skewing the response function in the positive and negative k_2 direction, respectively. The explanation for this is

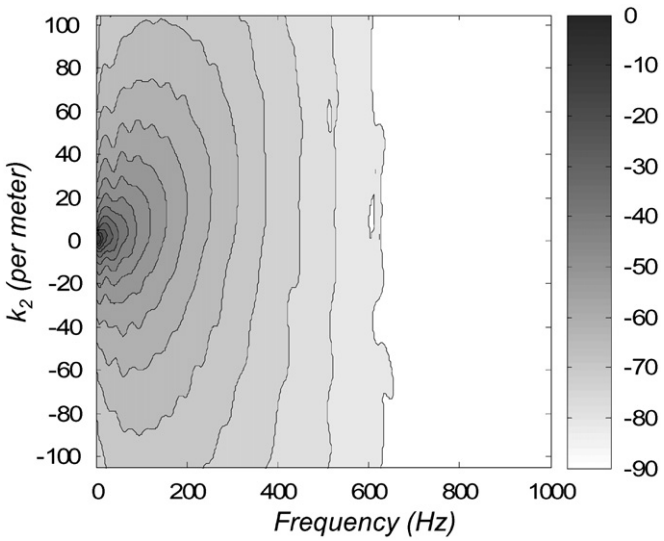

Fig. 13. Response function in wavenumber frequency space for the S831 airfoil at 0°. Scale is dB relative to maximum value.

straight forward if we consider the response function as it would be seen in physical space (e.g. Fig. 4b). Regardless of whether the airfoil is cambered or not its sensitivity to convected vorticity will always be largest just ahead of the leading edge because the airfoil is most effective in blocking the velocity field induced by the vorticity in this position. Furthermore, we would expect (based upon the Joukowski mapping result for a curved plate) that, regardless of camber, the flow at zero angle of attack will still stagnate very close to the airfoil leading edge. It therefore seems reasonable to expect that the stagnation streamline will still nearly evenly divide the most sensitive part of the response function leading, for example, to the unskewed distribution in Fig. 13. The implication is that in general camber, unlike angle of attack, will have a relatively weak effect on the airfoil response function.

5. Conclusions

Leading edge noise measurements have been made on a three airfoils (0.20 m chord NACA 0012, 0.61 m NACA 0015 and 0.91 m S831) immersed in closely homogenous isotropic turbulence. The airfoils included variations in chord, thickness and camber and the measurements encompass integral scale to chord ratios from 9 to 40 percent as well as 4:1 ratios of leading edge radius and airfoil thickness to integral scale. Calculations have been made using the panel method approach of Glegg and Devenport [2] that exactly accounts for the airfoil geometry. We find good agreement (typically within 2 dB or better) between measurement and prediction. We have therefore been able to use both measurement and prediction to reveal and understand some effects of thickness, angle of attack and camber on airfoil response and leading edge noise.

In all cases noise levels at high frequencies are substantially attenuated by the airfoil thickness, even for the NACA 0012 for which the airfoil thickness and leading edge radius are less than 1/3rd and 1/20th, respectively, of the turbulence integral scale. In general the attenuation increases with thickness but this effect is not a unique function of overall thickness or leading edge radius.

The effects of angle of attack on sound radiated by the two NACA foils are remarkably small, consistent with prior observations. Angle of attack effects on the airfoil response functions, produced by the distortion of the flow around the leading edge, are large but these effects are almost completely lost when the response function is averaged with the isotropic turbulence energy spectrum. The implication is that with a significantly different inflow turbulence spectrum or airfoil geometry significant angle of attack effects would be seen in the sound spectrum. This is found to be the case. Calculations performed for the NACA 0015 airfoil for the practically important case of anisotropic turbulence spectrum show an increase in sound levels of as much as 10 dB from 0° to 12° angle of attack. Calculations performed for the much different geometry of the S831 airfoil (in isotropic turbulence) show a significant decrease in sound levels with angle of attack.

The effects of camber on the airfoil response function have been discussed and appear likely to be small. Angle of attack effects on the response function of the strongly cambered S831 airfoil are shown to be centered on zero angle of attack, rather than the zero lift angle of attack. This occurs because the camber does not influence the extreme sensitivity of the airfoil to disturbances in the leading edge region or the stagnation of the flow upon that region at zero angle of attack.

Acknowledgments

The authors would like to thank the Office of Naval Research, in particular Dr. Ron Joslin, for their support under Grants N00014-05-1-0464 and N00014-04-1-0493. The support of NREL, in particular Drs. Pat Moriarty and Paul Migliore, in providing the 0.91 m chord airfoil models and in contributing to the development of the anechoic facility through Grant ZAM-4-33226-01 is gratefully acknowledged. The authors would like to thank Mr. Nathan Alexander for his assistance in taking some of the wind tunnel measurements presented here.

References

[1] P.F. Mish, W.J. Devenport, An experimental investigation of unsteady surface pressure on an airfoil in turbulence—Part 1: effects of mean loading, *Journal of Sound and Vibration* 241 (2006) 417–446.
[2] S.A.L. Glegg, W.J. Devenport, Panel methods for airfoils in turbulent flow, accepted for publication in *Journal of Sound and Vibration*, see also S. Glegg, W.J. Devenport, J. Staubs, Sound radiation from three dimensional airfoils in a turbulent flow, *Proceedings of 46th AIAA Aerospace Sciences Meeting*, Reno, NV, 2008, AIAA-2008-0052.
[3] G.L. Commerford, F.O. Carta, An exploratory investigation of the unsteady aerodynamic response of a two-dimensional airfoil at high reduced frequency, United Aircraft Research Laboratories, East Hartford, Connecticut, Report UAR-J182, 1970.
[4] S.R. Manwaring, S. Fleeter, Rotor blade unsteady aerodynamic gust response to inlet guide vane wakes, *Journal of Turbomachinery* 115 (1993) 197–206.
[5] I.J. Sharland, Sources of noise in axial flow fans, *Journal of Sound and Vibration* 1 (1964) 302–322.
[6] W. Olsen, J. Wagner, Effects of thickness on airfoil surface noise, *AIAA Journal* 20 (1982) 437–439.
[7] K.S. Aravamudan, W.L. Harris, Low frequency broadband noise generated by a model rotor, *Journal of the Acoustical Society of America* 66 (1979) 522–533.
[8] R.W. Patterson, R.K. Amiet, Acoustic radiation and surface pressure characteristics of an airfoil due to incident turbulence, *Proceedings of Third AIAA Aero-Acoustics Conference*, Palo Alto, CA, July 1976, AIAA 76-571. See also NASA CR2733.
[9] J.L. Gershfeld, Leading edge noise from thick foils in turbulent flows, *Journal of the Acoustical Society of America* 116 (2004) 1416–1426.
[10] S. Oerlemans, P. Migliore, Aeroacoustic wind tunnel tests of wind turbine airfoils, *Proceedings of 10th AIAA/CEAS Aeroacoustics Conference*, Manchester UK, May 2004, AIAA 2004-3042.
[11] S. Moreau, M. Roger, M.V. Jurdic, Effect of angle of attack and airfoil shape on turbulence interaction noise, *Proceedings of 11th AIAA/CEAS Aeroacoustics Conference*, Monterey, CA, May 2005, AIAA 2005-2973.
[12] P.J. McKeough, J.M.R. Graham, The effect of mean loading on the fluctuating loads induced on aerofoils by a turbulent stream, *The Aeronautical Quarterly* 31 (1980) 56–69.
[13] P.F. Mish, W.J. Devenport, An experimental investigation of unsteady surface pressure on an airfoil in turbulence—Part 2: sources and prediction of mean loading effects, *Journal of Sound and Vibration* 296 (2006) 447–460.
[14] K. Choi, R.L. Simpson, Some mean velocity, turbulence and unsteadiness characteristics of the VPI & SU stability wind tunnel, Department of Aerospace and Ocean Engineering, Virginia Tech, Blacksburg, VA, Report VPI-Aero-161, 1987.
[15] M. Remillieux, E. Crede, H. Camargo, R. Burdisso, W. Devenport, M. Rasnick, P. van Seeters, A. Chou, Calibration and demonstration of the new Virginia Tech anechoic wind tunnel, *Proceedings of 14th AIAA/CEAS Aeroacoustics Meeting*, Vancouver, BC, May 2008, AIAA-2008-2911.
[16] J. Staubs, Real Airfoil Effects on Leading Edge Noise, Ph.D. Dissertation, Virginia Tech, Available at ⟨http://scholar.lib.vt.edu/theses/available/etd-05282008-002246/⟩, May 2008.
[17] E. Crede, Aerodynamics and Acoustics of the Virginia Tech Stability Tunnel Anechoic System, M.S. Thesis, Virginia Tech, Available at ⟨http://scholar.lib.vt.edu/theses/available/etd-08112008-094223/⟩, June 2008.
[18] S. Bereketab, H. Wang, P. Mish, W.J. Devenport, The surface pressure response of a NACA 0015 airfoil immersed in grid turbulence. Volume 1: characteristics of the turbulence, Final Report to NASA Langley under Grant NAG 1-1942, 2000.
[19] R.K. Amiet, Acoustic radiation from an airfoil in a turbulent stream, *Journal of Sound and Vibration* 41 (1975) 421–432.
[20] E.J. Kerschen, P. Gliebe, Fan noise caused by the ingestion of anisotropic turbulence—a model based on anisotropic turbulence theory, *Proceedings of Sixth AIAA Aeroacoustics Conference*, Hartford, CT, June 1980, AIAA-1980-1021.
[21] E.J. Kerschen, P. Gliebe, Noise caused by the interaction of a rotor with anisotropic turbulence, *AIAA Journal* 19 (1981) 717–723.
[22] G.K. Batchelor, *The Theory of Homogeneous Turbulence*, Cambridge University Press, Cambridge, 1953.
[23] W. Devenport, R. Burdisso, H. Camargo, E. Crede, M. Remillieux, M. Rasnick, P. van Seeters, Aeroacoustic testing of wind turbine airfoils, Final Report to NREL under Contract 208-11-110F-101-408-1, AOE Department, Virginia Tech.